Digest Journal of Nanomaterials and Biostructures Vol. 12, No. 4, October-December 2017, p. 1187-1196

CHARACTERIZATION OF CuPcTs/PS for NO_2 GAS SENSOR

I. M. IBRAHIM[a], J. M. RZAIJ[b], A. RAMIZY[b, c]
[a]*Department of physics, College of Science, Baghdad University, Baghdad, Iraq*
[b]*Department of physics, College of Science, University of Anbar, Anbar, Iraq*
[c]*Renewable energy Research Center, University of Anbar, Anbar, Iraq*

This work reviews the use of porous silicon (PS) (P-type) as a nanomaterial which is extensively investigated and utilized for metal-deposition within the porous structures. Emphasis will be put on self-arranged mesoporous silicon, offering a quasi-regular pore arrangement, employed as template for filling with Copper phthalociyanine Tetraselfonic acite tetraselfonic salt (CuPcTs) organic semiconductor. AFM images show decreasing in average diameter with increasing of etching current from 10 mA to 50 mA. The optical absorption spectrum of the CuPcTs film shows the absorption peaks of B and Q bands at around 330 and 620 nm, while for annealing samples the peaks shifted to 337 and 578 for B and Q respectively. The scanning electron microscopy of all films of CuPcTs reveals nano grain size with diameter less than 100 nm. The sensitivity is reduced gradually with increasing of operating temperature. Among all the values of etching current, a 40 mA exhibit the peak sensitivity of 98% at 50^0C operating temperature. The response value (S) of film to 100 ppm NO_2 was 12sec. Furthermore, fast recovery rate, long-term stability were also observed over a concentration range from 5 to 100 ppm.

(Received September 13, 2017; Accepted December 5, 2017)

Keywords: Porous Silicon, Phthalocyanine, Nitrogen dioxide sensors

1. Introduction

Porous silicon can be considered as a silicon crystal having a network of voids in it. The nano sized voids in the bulk silicon result in a sponge-like structure of pores and channels surrounded by a skeleton of crystalline Si nano wires. Porous silicon (PS) is gaining scientific and technological attention as a potential platform mainly for its multifarious applications in sensing and photonic devices(Pavesi & Dubos ; 1997; Tsamis et al., 2002; Archer & Fauchet, 2005; Barillaro et al.,2003)[1-4] The extremely large surface to volume ratio ($500m^2/cm^3$) of PS, the ease of its formation, control of the surface morphology through variation of the formation parameters and its compatibility to silicon IC technology leading to an amenability to the development of smart systems-on-chip sensors have made it a very attractive material[5]. Due to these multifunctional applications of PS, recently it has been proposed to be an educational vehicle for introducing nanotechnology and inter-disciplinary material science by eminent scientists working in this field. Therefore passivation of surface is necessary to make stable porous silicon based devices. For that purpose substituting surface hydrogen by another chemical species has appeared desirable. Oxidations (Rossi et al, 2001; nitradation (Anderson et al., 1993) and halogenation (Lauerhaas & Sailor, 1993) are found to be useful for PS surface passivation[6-8]. Derivatisation by organic groups and polymer (Lees et al. 2003; Mandal et al. 2006)[9,10].

The importance of environmental gas monitoring is well understood and much research has focused on the development of suitable gas-sensitive materials. Recently, there has been considerable interest in exploiting organic substances such as porphyrin [11], phthalocyanines [12,13]. The organic semiconductors are good candidates for the elaboration of chemical or electrochemical sensors in two main ways. (1) As sensitive components: The electronic conductivity related to the redox state (doping level) of a conducting organic

*Corresponding author: asmat_hadithi@uoanbar.edu.iq

semiconductor is modulated by the interaction with various substrates. Changes in parameter values, such as resistance, current or electrochemical potential, give a straight forward sensor response of the studied phenomena. (2) As a matrix for specific immobilization: Conducting polymers are often infusible and insoluble. Consequently, immobilization by entrapment of specific molecules that are capable of substrate recognition can be carried out mainly during polymerization process. However, this growing reaction added to the entrance of negatively charge species (sometimes positive ones) makes it possible to entrap various moieties easily in a one step process, with the further advantages of intrinsic porosity and electronic accessibility [14,15].In its simplest form, if a particular vapor is absorbed by the film and affects the conductivity, its presence may be detected as a conductivity change. The first evaluation of organic semiconductors as sensitive components in chemical sensors are based on their redox interaction with some gases, including a variation of the doping level, resulting in a quite straight forward conductance, monitoring of gas sensor response over orders of magnitude [16]. The observation that the semiconducting properties of phthalocyanine are modulated by the absorption and desorption of gases has led to significant efforts toward their incorporation in chemical sensors. It is hoped that making appropriate substitutions of metals in the cavity and organic substituents at the periphery of the phthalocyanine structure may develop the gas specificity.

In this study, an organic compound Copper (II) phthalocyaninetetrasulfonic acid tetrasodium salt (CuPcTs) has been prepared on glass and PS substrates. Porous silicon and its combination with CuPcTs leads to nanocomposites with specific physical properties caused by the nonometric size and give rise to a multiplicity of potential applications for chemical vapors of nitrogen dioxide sensor devices.

2. Experimental work

Porous silicon is generated by the electrochemical etching process (ECE) of p-type <100> oriented silicon substrate. The ECE cell was made of Teflon (or any highly acid-resistant polymer) base plate was made of aluminum. A Si wafer cut into a pieces with a square shape at area 1cm^2 and put on the bottom of the cell by using O-ring that allowed the Si surface to be exposed to the homogeneously mixed of HF: ethanol at 1:1 concentration. Si wafers were ultrasonically cleaned in distilled water and acetone, connected to the anode electrode and the Platinum connected to cathode electrode of the power supply as shown in Figure 1. PS samples were fabricated by changing the etching current density (10-50 mA) with a constant etching time (10mn).

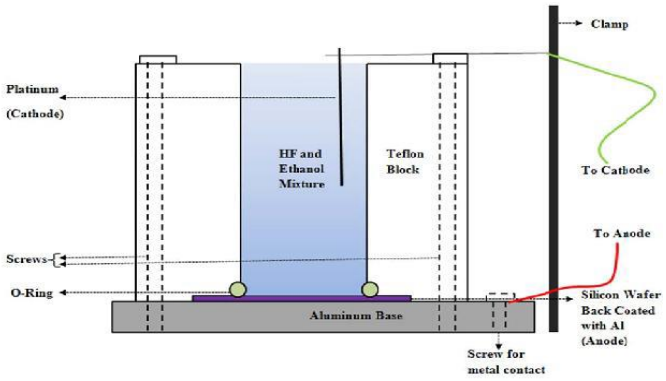

Fig. 1. Setup for the fabrication of porous silicon

Copper (II) phthalocyaninetetrasulfonic acid tetrasodium salt (CuPcTs) was purchased from Sigma-Aldrich and used without further purification. Its molecular formula is ($C_{32}H_{12}CuN_8O_{12}S_4Na_4$) and has 984.25 g/mol molecular weight. Molecular structure of CuPcTs is shown in Fig. (2), before starting the deposition, the glass substrate was put in an ultrasonic bath

for 15 min using alcohol then acetone, followed by cleaning in distilled water. The substrate was dried in open air in a cleaned room.

CuPcTs powder has mixed with deionized water 30mg/ml to obtain CuPcTs Solution then it has put on a magnetic stirrer for 15min. after that Filtration process is used to the mixture by using 0.2µm filters. And it has put on a magnetic stirrer for 30min to get a Homogenous solution. The resistivity of the used deionized water was ~15 MΩ-cm

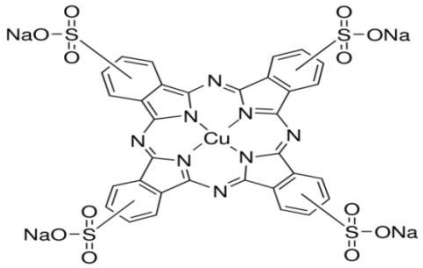

Fig. 2. Molecular structure of Copper (II) phthalocyaninetetrasulfonic acid tetrasodium salt (CuPcTs)

In this research work, a good uniform CuPcTs films can be obtained from the CuPcTs solution by spin coating at a spin rate of 1500 rotations per minutes (rpm). to get thickness thin films (40-60) nm Au electrodes were deposited on the CuPc alternate LbL film surface by a vacuum evaporation method in order to measure the sensing properties. The gap between the electrodes was 20 µm. Figure 3 shows the schematic diagram of CuPcTs/PS with gold mesh as electrode.

Field emission scanning electron microscopy (FESEM) type Hitachi S-4160 Japan Daypetronic Company, which is used to get topographical and elemental information at magnifications of 10 X to 300,000 X, with virtually unlimited depth of field.

The UV–Vis absorption spectra of the fabricated films were observed using a spectrophotometer (USB2000, Ocean Optics). Thicknesses of the deposited films on PS wafer were obtained using ellipsometry (Multiskop, Optrel GbR). He–Ne laser beam with wavelength of 632.8 nm was used for the ellipsometry measurement. Atomic force microscopy (AFM) imaging was performed in air using a Nanoscope IIIa system (Digital Instruments). Platinum (Pt) metal contact with a thickness of 200 nm was deposited onto the surface of of CuPcTs/PS using the sputtering system to fabricate the gas sensor as shown in figure 3.

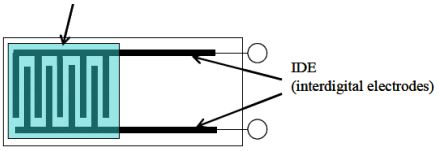

Fig. 3. Schematic diagram of CuPcTs/PS gas sensor

3. Results and discussion

Fig. (4) shows AFM images of PS at constant time of 10 min and different etching current from 10 mA to 50 mA. The surface morphology of the oxidized PS layers was investigated using AFM focus entirely on the nano scale characterization of PS. A sponge-like structure is produced. When current density increases, a part of pores coagulate to larger structures. The irregular and randomly distributed nano crystalline silicon pillars and voids over the entire surface can be recognized using the 3D images of AFM. The progress of the etching process was limited, therefore, the uniform pore on the wafer was created. Also the effect of H bubbles that created at the surface of the sample lead to reduce of HF concentration, thus preventing further silicon

dissolution **[17]**. The parameters of AFM, such as average diameter, peak–peak for these samples have been shown in the table (1). This table shows an increment in average diameter with increasing of etching current from 10 mA to 50 mA.

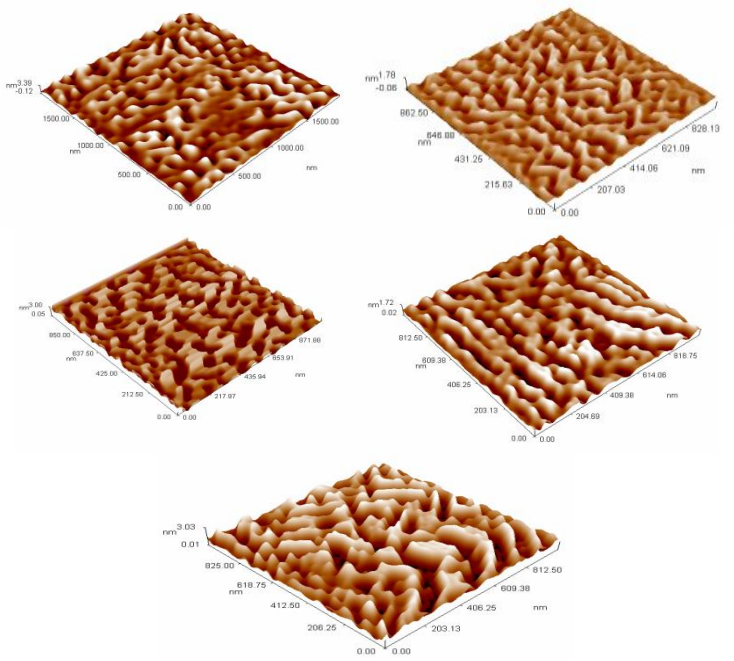

Fig. 4. Atomic force microscopy of p-type Si(111) in three dimensions at different etching current a)10mA b)20mA c)30mA d)40mA and e) 50mA

Table (1) AFM parameters for porous silicon with constant time and different etching current (10, 20, 30, 40 and 50) mA.

Etching current (mA)	Avg. Diameter (nm)	Peak-Peak (nm)
10	92.63	1.7
20	85.90	1.7
30	62.29	2.29
40	61.62	3.51
50	54.91	4.9

FTIR- spectrum of CuPcTs:

CuPcTs was measured in the infrared range 500-3500 cm^{-1} to identify the type and position of the bonds, Figure (5) shows the FTIR transmission of CuPcTs compound .

FTIR characteristic absorption bands at 3464.4, 3055.61, 1336.32, 1195.2, 1608.79 and 681.54 cm^{-1}, the bond bending represented by the range (1320-1334) cm^{-1} and the bond stretching represented by the range (3033-3300) cm^{-1} [see table 2]. The thin films show peaks at (500- 700) cm^{-1}, originate most probably from vibrations in the benzene rings. The FTIR spectrum of CuPcTs has a typical vibration modes such as peak at 3464.4 cm^{-1} which is attributed to non-planer deformation of C-H bonds of benzene rings, there is a peak at 3055.32 cm^{-1} which have been assigned for bond of N-H stretching bands, peak at 1608.79 cm^{-1} for bond of C=C for bending bond, peak at 1336.32 cm^{-1} for bond of C-N, this result has good agreement with M. T. Hussien [18] .

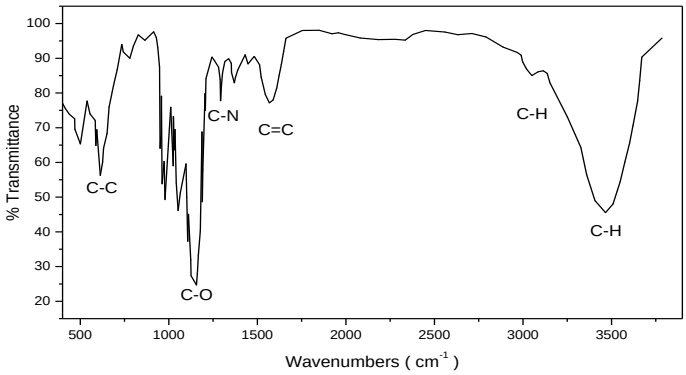

Fig. 5. FTIR spectrum of CuPcTs compound.

Table 2. The peak positions and bonds of CuPcTs

Functional group	Peak position(cm-1)	Peak Position ref (cm^{-1})	Bonds	Attribution
C-H	3020	3033-3300	C-H	Stretching
C-N	1303	1320-1334	C-N	Bending
C-O	1125.20	1195	C-O	———
C=C	1608.79	1608	C=C	Macrocycle ring deformation
C-C	613.54	617	C-C	Out-of-plan deformation

The optical absorption spectrum of the CuPcTs films on glass substrates was measured and is shown in Fig. 6 and Q bands were observed to be 1.55eV and 3.05eV, respectively. It was found that the deposition of CuPcTs was successful. In the Q band, an intense absorption peak at 620nm is due to the transition between the bonding and antibonding (π-π*) at the dimer part of the phthalocyanine molecule. Copper atom of the phthalocyanine molecule is associated with the *d*-band. Therefore, within the UV region of the spectrum, a strong absorption peak at 330nm is attributed to partially occupied *d*–π* transitions. The variations in absorbance with annealing temperature for B band are greater than the variations in Q band.

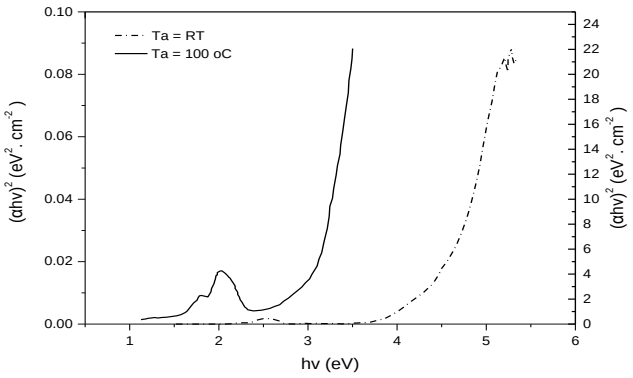

Fig.6 Tauc plot for CuPcTs thin film at room temperature and t annealed at 100 ^{o}C

The CuPcTs/PS films were characterized by scanning electron microscopy (SEM) images. The scanning electron micrographs of CuPcTs/PS at room temperature and annealed at 100 ^{0}C

are shown in Fig (7). The film morphology changes for the elevated annealing temperatures. All films of CuPcTs transformed into Nano grain size with diameter less than 100 nm as appeared in Fig. (7).This phenomenon indicates that the film preferentially grows parallel to the surface; this means that the grains are parallel to the substrate surface and they became Nano as the annealing temperature increased. It is also observed that the shapes of grain like islands are separated from each other at higher temperature. The same results are found in [19]

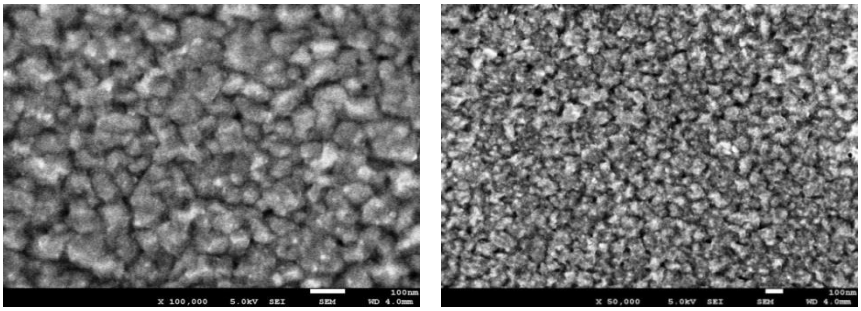

Fig.7. SEM pictures of CuPcTs Film deposited on PS at RT and 100^{o}C

NO_2 sensing mechanism for CuPcTs /PS

CuPcTs /PS gas sensing properties of films prepared on porous silicon (PS) at different etching current for the detection of NO_2 gas with concentration of 100ppm. Sensing behavior was examined at room temperature, 50 and 100 ^{0}C operating temperatures.

Fig. (7) shows the variation of resistance as a function of time with on/off gas valve. The result shows decreasing in the resistance value when their films were exposed to NO_2 gas, (Gas ON), then the resistance value back upward at the closure of the gas (Gas OFF). The reason for this behavior can be attributed to the following: p-type semiconductor is a material that conducts with positive holes being the majority charge carriers, NO_2 gas undergoes an ionic reaction with the surface adsorption oxygen, where the electron on the oxygen, is extracted from the semiconductor and causes the conductivity of the CuPcTs materials to increase, thus causing the resistance to decrease. The sensitivity factor (S %) at various temperatures is calculated by equation [20]:

$$S = \left| \frac{(R_g - R_a)}{NR_a} \right| \times 100\% \qquad (1)$$

Where (R_a) and (R_g) are the electric resistance of the sensor in air and in presence of gas respectively and (N) is the gas concentration

The films sensitivity increases as the operating temperature increased from room temperature to 100°C due to thermal excitation of the charge carriers in semiconductors. When the temperature exceeds 100°C, the film sensitivity is slowly increased. This can attributed to the saturation of the conduction band with electrons elevate from shallow donor levels caused by oxygen vacancies.

The high sensitivity may be attributed to the optimum surface roughness, porosity and large surface area. Among all the values of etching current a 40 mA exhibit high sensitivity of 98% at 50^{0}C operating temperature[21].

The observed response time of the film to 100 ppm NO_2 was 12sec. Furthermore, fast recovery rate, good reproducibility and acceptable long-term stability were also observed over a concentration of 100 ppm. The outstanding sensing performance may be attributed to the porous roughness, ultra-thin film structure and the "NO_2capture" effect of the "flickering" CuPcTs molecules. Therefore, the proposed CuPcTs/PS thin film sensors are excellent potential candidates for NO_2 detection.

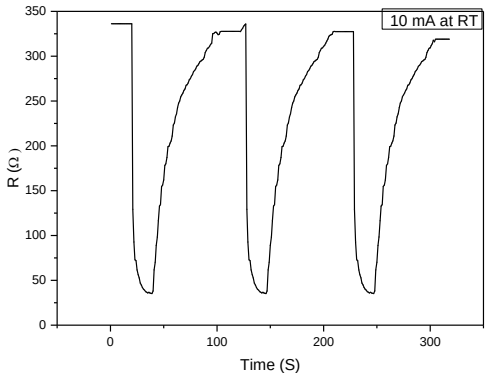

a) *at RT with etching current of 10 mA.*

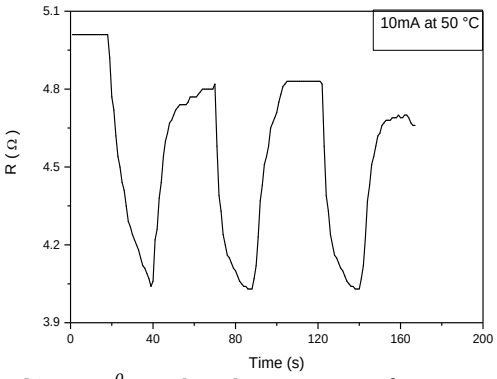

b) *at 50 ^{0}C with etching current of 10 mA.*

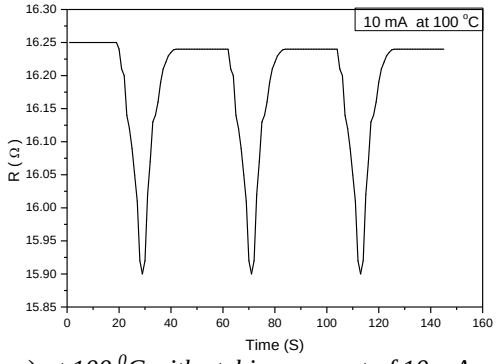

c) *at 100 ^{0}C with etching current of 10 mA.*

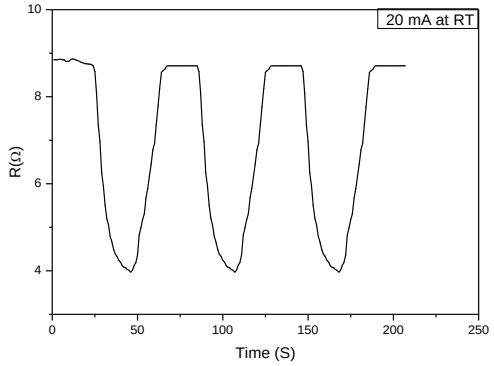

d) *at RT with etching current of 20 mA.*

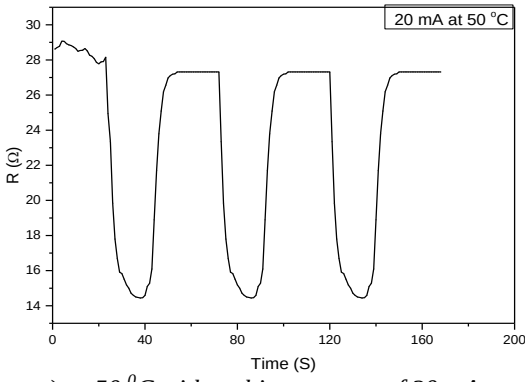

e) *at 50 ^{0}C with etching current of 20 mA.*

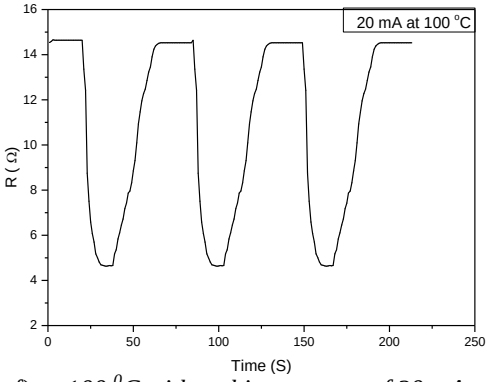

f) *at 100 ^{0}C with etching current of 20 mA.*

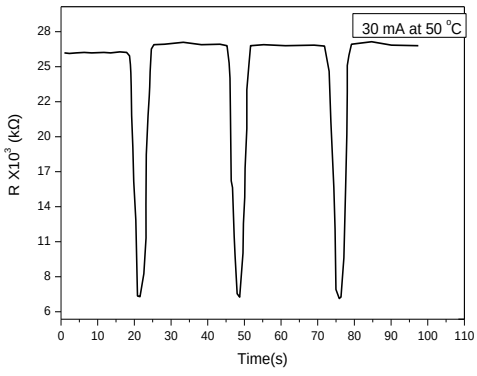

g) *at RT with etching current of 30 mA.*

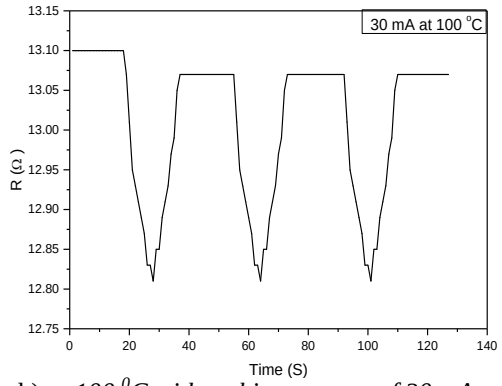

h) *at 100 ^{0}C with etching current of 30 mA.*

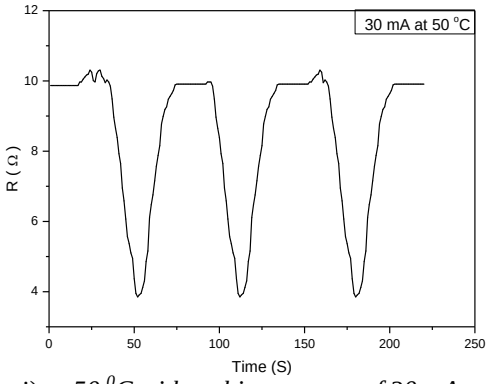

i) *at 50 ^{0}C with etching current of 30 mA.*

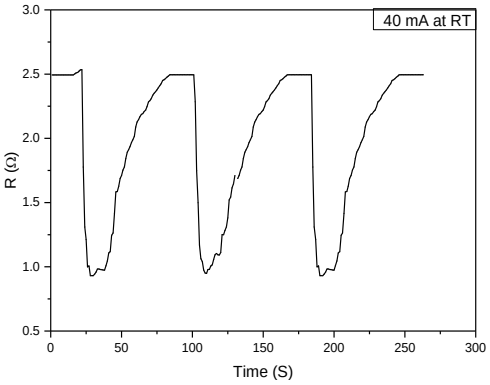

j) *at RT with etching current of 40 mA.*

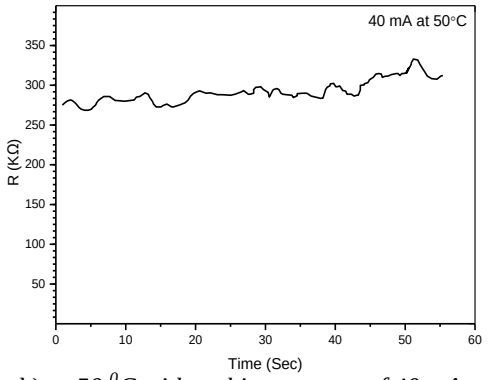

k) *at 50 ^{0}C with etching current of 40 mA.*

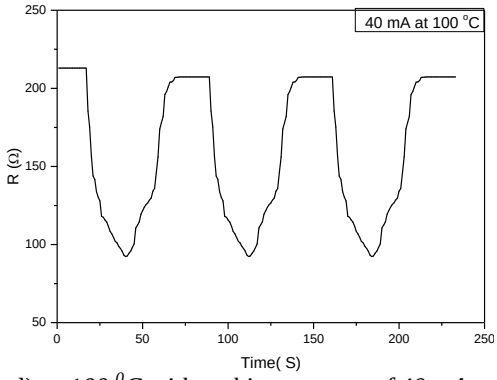

l) *at 100 ^{0}C with etching current of 40 mA.*

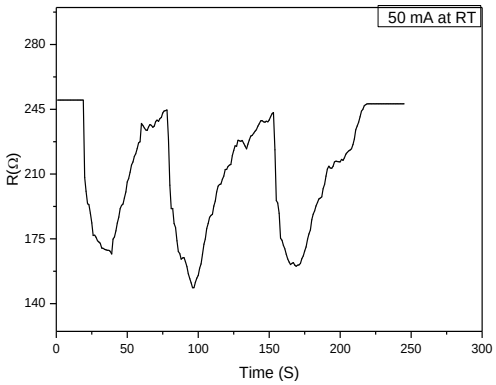

m) *at RT with etching current of 50 mA.*

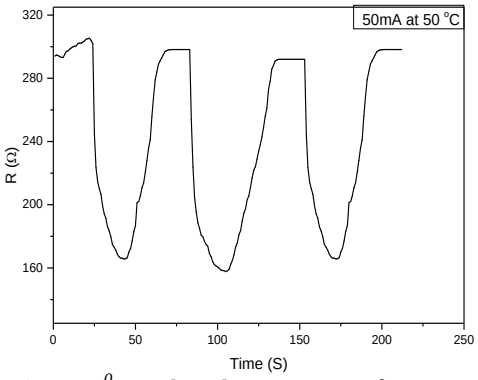

n) *at 50 ^{0}C with etching current of 50 mA.*

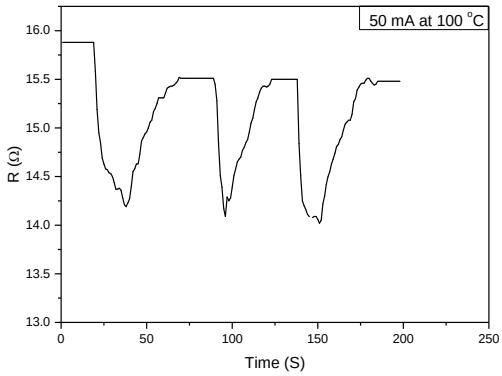

o) *at 100 ^{0}C with etching current of 50 mA.*

Fig.8 Sensitivity of CuPcTs /PS at different temperature and different etching current time.

Table 3. the sensitivity, Response and recovery time of CuPcTS/PS gas sensor at different etching current (10, 20, 30, 40 and 50 mA)

Samples at etching current (mA)	Sensitivity % at			Response time (s) at			Recovery time (s) at		
	RT	50 ^{0}C	100 ^{0}C	RT	50 ^{0}C	100 ^{0}C	RT	50 ^{0}C	100 ^{0}C
10	68	56	90	20	20	16	25	25	27
20	44	73	81	9	13	15	37	32	18
30	90	47	51	17	13	14	25	44	31
40	90	98	87	11	12	20	16	15	40
50	49	53	25	20	20	12	60	28	29

4. Conclusions

CuPcTs/PS (p-type) was prepared by spin coating technique. The optimum condition for porous silicon was at etching current 40mA. The highest response time of NO_2 gas sensor fabricated based on CuPcTs/PS was at etching current of 40mA and operating temperature of 50 ^{0}C. The results in this work are useful for the development of a highly sensitive gas sensor.

References

[1] L. Pavesi, P. Dubos, Semicond Sci and Technol. **12**, 570 (1997).
[2] C. Tsamis, L. Tsoura, A.G. Nassiopoulou, A. Travlos, C.E. Salmas, K.A. Hatzilyberis, G. P. Ndroutsopoulos, IEEE Sensors Journal **2**, 89 (2002).
[3] M. Archer, M. Christophersen, P. M. Fauchet, Sens. Actuators B **106**, 347 (2005).
[4] G. Barillaro, A. Nannini, F. Pieri, Sensors. Actuators, B **93**, 263 (2003).
[5] I. Porous, B. Laboratories, U. Goesele, Fundamentals of Porous Silicon Preparation (2012)
[6] A. M. Rossi, G. Amato, V. Camarchia, L. Boarnio, S. Borini, Appl. Phys. Lett. **78**(20), 3003 (2001).
[7] R. C. Anderson, R.S. Muller, C.W. Tobias, J.Electrochem.Soc. (USA) **140**, 1393 (1993).
[8] J.M. Lauerhaas, M.J. Sailor, Mat. Res. Soc. Symp. Proc. (USA), **298**, 259 (1993).
[9] I.N. Lees, H. Lin, C.A. Canaria, C. Gurtner, M.J. Sailor, G.M. Miskelly, Langmuir **19**, 9812 (2003).
[10] N. P. Mandal, A. Sharma, S. C. Agarwal, J.Appl.Phys. **100**, 024308 (2006).
[11] D.G. Zhu, D.F. Cui, M. Harris, M.C. Petty, Sensors & Actuators **12**, 111 (B 1993).
[12] J.D. Wright, P. Roisin, G.P. Rigby, R.J.M. Nolte, S.C. Thorpe, Sensors & Actuators, **13-14**, 276 (B 1994).
[13] P.S. Vukusic, J.R. Sambles, Thin Solid Films **221**, 311 (1992).
[14] Bartlett, P.N.; Liang-chung, S.K..(1989) Sensors & Actuators, 20, 287.
[15] S.Radhakrishnan, S. D. Deshpande, Conducting Polymers Functionalized with Phthalocyanine as Nitrogen Dioxide Sensors, Sensors **2**, 185 (2002).
[16] C. Nylander, M. Armgarth, I. Lundstrom, Anal. Chem. Symp. Ser. **17**, 203 (1983).
[17] U. R. I. Virgili, C. Of, P. Silicon, M. Optical, Des. Fabr. Charact. Porous Silicon Multilayer Opt. Devices. (2007)
[18] M. T. Hussein, "Theoretical IR spectroscopic study of Copper Phthalocyanine (CuPc)", **11(**2), 303 Baghdad (2008).
[19] B. Joseph, C. Menon, E-Journal of Chemistry **4**(2), 255 (2007).
[20] C. J. L. S. J. Kim, S. H. Lee, J. Phys. D Appl. Phys **34**, 3505 (2001).

[21] S. Rout, “Synthesis and Characterization of CuO/graphene oxide composite,” National Institute of Technology, Rourkela. (2012)